



ECOSYSTEMS

The use of sentinel-2 imagery to generate vegetations maps for the Northern Antarctic peninsula and offshore islands

ELIANA L. DA FONSECA, EDVAN C. DOS SANTOS, ANDERSON R. DE FIGUEIREDO & JEFFERSON C. SIMÕES

Abstract: We used Sentinel-2 imagery time series to generate a vegetation map for the Northern part of the Antarctica Peninsula and offshore islands, including the South Shetlands. The vegetation cover was identified in the NDVI maximum value composite image. The NDVI values were associated with the occurrence of algae (0.15 – 0.20), lichens (0.20 – 0.50), and mosses (0.50 – 0.80). The vegetation cover distribution map was validated using the literature information. Generating a vegetation map distribution on an annual basis was not possible due to high cloud cover in the Antarctic region, especially in coastal areas, so optical images from 2016 to 2021 were necessary to map the vegetation distribution in the entire study area. The final map analyzed in association with the weather data shows the occurrence of a microenvironment over the western islands of the Antarctic Peninsula that provided vegetation growth conditions. The Sentinel-2 images with 10m spatial resolution allow the assembly of accurate vegetation distribution maps for the Antarctica Peninsula and Islands, the Google Earth Engine cloud computing being essential to process a large amount of the satellite images necessary for processing these maps.

Key words: Biological soil crusts, Google Earth Engine, Microenvironments, South Shetland Islands, Vegetation cover, Spectral profiles.

INTRODUCTION

The vegetation in the Antarctic environment is restricted to ice-free areas, mainly in Antarctic islands and coastal regions of the continent (Alberdi et al. 2002, Convey 2006, Fretwell et al. 2011). These plant communities are predominantly cryptogamic, also known as lower plants or biological soil crusts (BSC), mainly mosses, algae, and lichens (Colesie et al. 2023) (Figure 1). Their growth season length depends on the climatic conditions, latitude, and relief (Selkirk & Skotnicki 2007). The availability of liquid water is the most critical factor for the development of vegetation communities in Antarctica, which is available only in summer

months, when the solar radiation reaches the Antarctic surface and in this brief period the snow melts, and rain occurs and the vegetation can absorb the humidity directly from the air (Elster 2002, Bölter et al. 2002, Choi et al. 2015).

The Antarctic vegetation is characterized by its seasonality, presenting a complex cycle, related with a set of environmental factors that influence the propagation, germination, growth, the formation of spores and propagules, as well as the establishment of cryptogamic communities (Lewis-Smith 2007). The Antarctic flora consists mainly of inferior plants, with occurrence of cyanobacteria, terrestrial and aquatic algae (700 species), bryophytes - mosses (100 species)

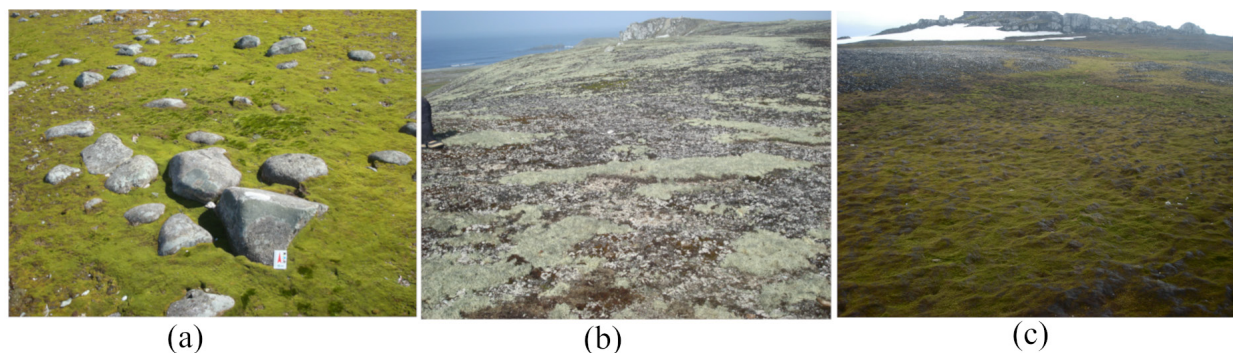


Figure 1. Harmony Point (Nelson Island), photographs showing different biological soil crusts: mosses (a), lichens (b), and algae (c).

and liverworts (25 species) and lichens (250 species) and only two species of vascular plants (grasses) (Alberdi et al. 2002, Peat et al. 2007). The environmental factors such as temperature, snow cover, winds, daylength, anthropogenic activity and the presence of animals also affect the growth and spatial distribution of vegetation in the maritime Antarctic (Alberdi et al. 2002).

Terrestrial macroscopic green algae in Antarctica occur on ice-free surfaces. Few terrestrial algae can have their biomass visually identified; among them are *Prasiola* spp. and *Nostoc* spp. (Broady 1996, Elster 2002). The genus *Prasiola* is considered one of the most important primary producers in the Antarctic environment. Their growth is generally associated with moist and biogenic soils, coastal spray zones above the coast, and areas of penguin nests and their surroundings (Becker 1982, Jacob et al. 1991, Brody 1996, Moniz et al. 2012). They are tolerant to freeze-thaw during spring and autumn and high incident radiation rates in the Austral summer (Moniz et al. 2012). The mosses communities were identified in different environments where water is available during the Austral summers (Lovelock & Robinson 2002) and are the dominant element of the vegetation (Cannone et al. 2017) due to their well-developed stress tolerance features (Colesie et al. 2023). Lichen communities are dispersed

over a variety of habitats, such as exposed or protected areas from the winds or with bare rock and stable substrate surfaces (Kappen 2000, Lovelock & Robinson 2002), and also as the fellfield ecosystems generally dominated by several communities of lichens (Lewis-Smith 2007). The lichen species always present a slow growth rate related to the short-term favorable environmental conditions (Sancho & Pintado 2004); their cells do not have water-conducting tissues, so they are directly exposed to humidity conditions (Kappen & Schroeter 2002).

The use of remote sensing to map the Antarctic vegetation has generated few maps at local scales, mainly in areas frequently visited by researchers (Calviño-Cancela & Martín-Herrero 2016), usually by very-high-resolution images collected by orbital sensors, such as KOMPSAT-2 and QuickBird (Shin et al. 2014) and WorldView-2 (Jawak et al. 2019) and by Unmanned Aerial Vehicles (UAV) (Miranda et al. 2020, Sotille et al. 2020). These studies primarily focused on detecting the presence/absence of vegetation using the Normalized Difference Vegetation Index (NDVI) to generate maps with information valid only for the time of the image acquisition, usually made only once during the entire vegetation growth season.

At regional scales, Fretwell et al. (2011), mapped the probability of vegetation occurrence

for the Antarctic Peninsula, based on the Landsat Image Mosaic of Antarctica (LIMA mosaic), with images acquired in 2007–2008. In recent literature, the Antarctic vegetation is not considered in global forecasts (e.g., Jung et al. 2021) due to the lack of information on this region. A vegetation map can be used as an input layer in simulations of environmental changes processes, such as climate variables or carbon sinks, and can be analyzed by its content. Mapping the current Antarctic vegetation distribution is required to understand the impact of these changes on vegetation biomass accumulation and the greenhouse gas cycle in the near future. This work aimed to generate a vegetation map for the northern part of the Antarctica Peninsula, offshore islands and the South Shetland Islands (Figure 2) based on Sentinel-2 imagery time series using the Google Earth Engine (GEE) data catalog and cloud processing. In this paper, we describe the steps for the automatic process and their theoretical background to generate a vegetation map using the cloud processing of “ready analysis” Sentinel-2 imagery.

MATERIALS AND METHODS

All the processes were made in Google Earth Engine GEE (Gorelick et al. 2017) using its native JavaScript interface, accessed by Google Chrome. The cartography was produced using QGIS and ESRI satellite base map, available at Quickmap services plugin. Figure 3 shows a flowchart with the main steps to generate the vegetation map, which are fully explained in the following sections. These studies primarily focused on detecting the presence/absence of vegetation using the Normalized Difference Vegetation Index (NDVI) to generate maps with information valid only for the time of the image acquisition, usually made once during the entire vegetation growth season.

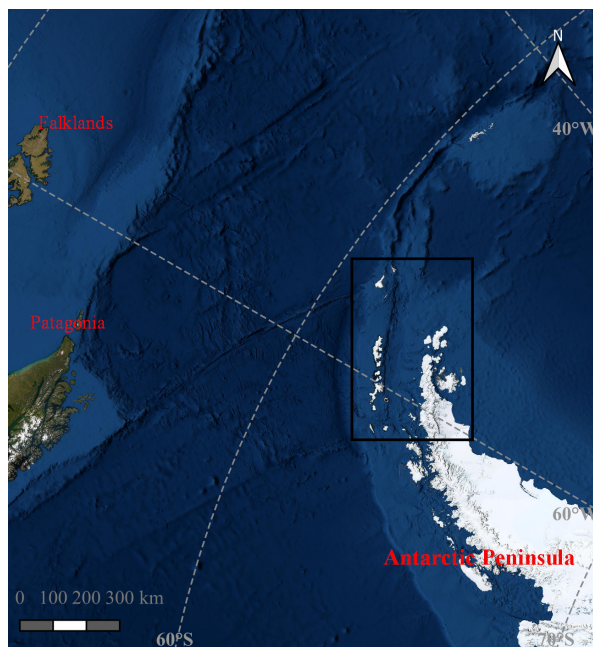


Figure 2. This study area, the northern part of the Antarctic Peninsula and the South Shetland Islands (black rectangle) over an ESRI satellite base map.

NDVI labels based on the vegetation types

Vegetation type identification for each NDVI value range was necessary for labeling the NDI classes. This labeling was made using a Sentinel-2 image acquired on February 23, 2019, from the Surface Reflectance Sentinel-2 collection (COPERNICUS/S2_SR), available in the GEE data catalog as a ready-to-use product. The Surface Reflectance Sentinel-2 collection data came from the European Union/ESA/Copernicus, which contains the surface reflectance values (orthorectified and radiometrically corrected at the surface) calculated for each Sentinel-2 spectral band and three QA bands (quality assessment). We chose to use surface reflectance data due to the availability of information in the literature on surface reflectance data for identifying BSC targets. We also considered the availability of a Sentinel-2 cloud-free image covering Harmony Point, Nelson Island (Figure 4), for the same month of the fieldwork

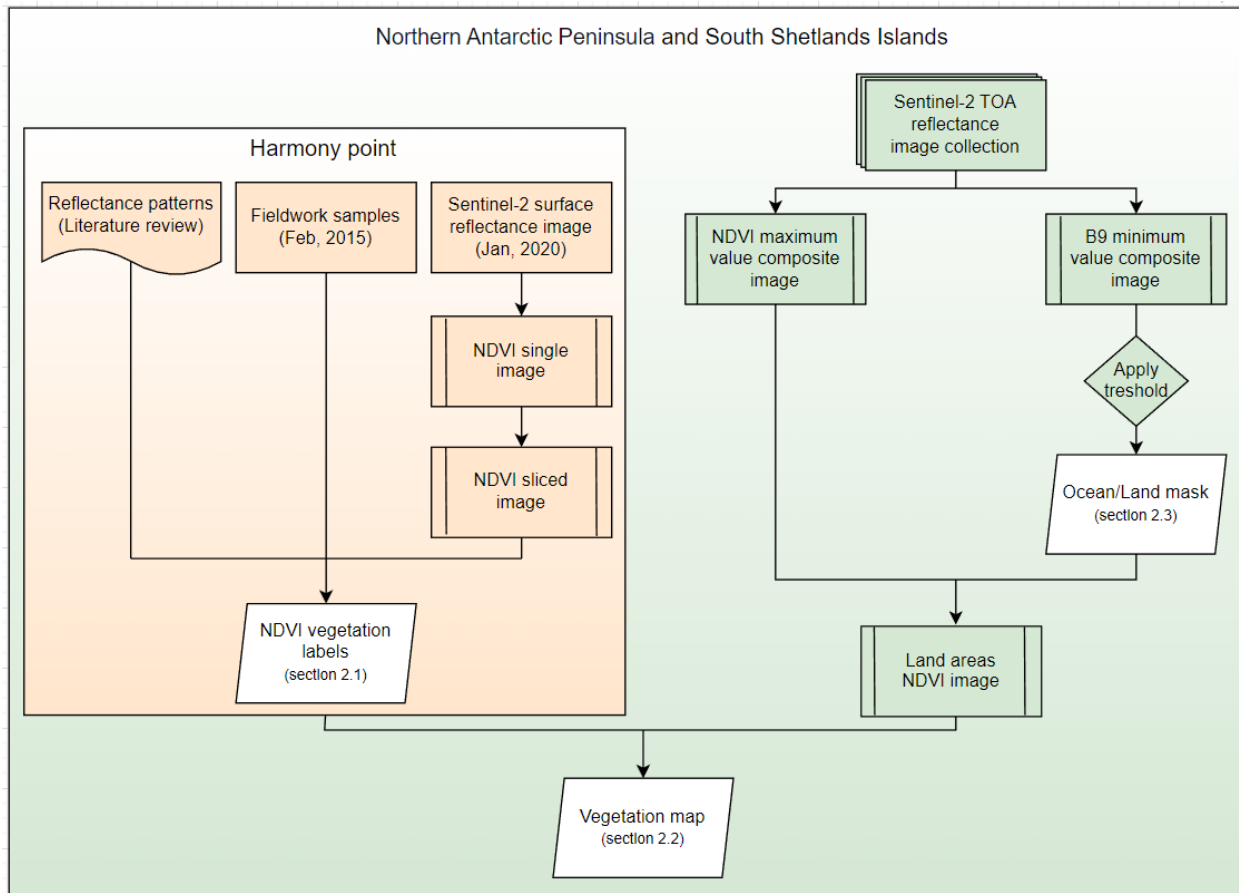


Figure 3. Flowchart with the main steps to generate the NDVI labels, the ocean/land mask and the vegetation map.

(February 13-20, 2015). At that time, we collected information about vegetation cover type, *i.e.*, algae, lichens, or mosses (Figure 1), in 17 sample points in Harmony Point (Figure 4). These points were used associated with literature information to label the NDVI classes.

An NDVI image was calculated using red and near-infra-red wavelengths (B4 and B8), with 10 meters spatial resolution. The NDVI values range between -1 and 0 for water, ice, clouds, and clouds shadows and between 0 and 1 for bare areas and vegetation. The positive NDVI values were sliced every 0.05, generating twenty NDVI bins. The mean surface reflectance values for each Sentinel-2 spectral band located at blue, green, red, red-edge, NIR, and SWIR wavelengths were collected for all the pixels in each NDVI bin.

Their values were compared with those in the literature for BSC surface reflectance patterns (Lovelock & Robinson 2002, Zhang et al. 2007, Chi et al. 2021). Also, the NDVI bins were related to fieldwork information by the overlap of the NDVI image and the sample points' locations to label the NDVI values as lichens, mosses, or algae.

Vegetation maps from NDVI images

We composed the vegetation map using a Sentinel-2 level 1C time series imagery (orthorectified and radiometrically corrected at the top-of-atmosphere - TOA reflectance), available in the GEE (“COPERNICUS/S2” collection) acquired by Sentinel 2A and 2B over the northern part of the Antarctic Peninsula, its



Figure 4. Samples points locations at Harmony Point in Nelson Island, South Shetland Islands.

surrounding islands and the South Shetland Archipelago from 2016 until 2021. This collection contains the TOA reflectance values calculated for each Sentinel-2 spectral band and quality assessment (QA) bands as ready-to-use products. The TOA reflectance product, available in the GEE, was used instead of the surface reflectance product since the labeling process is done by comparing the reflectance patterns of different targets. Over the Antarctica region, there are few available surface reflectance images in the Sentinel-2 image collections. Due to the high spectral absorption and scattering of ocean optical constituents in this region, the

atmospheric correction models in coastal areas do not work properly (Warren et al. 2019).

Eleven subsets were created to generate the vegetation maps (four for the northern Antarctic Peninsula – south, north, north, and west islands – and seven for the South Shetlands – Elephant and Clarence, King George, Nelson, Robert, Livingston, Deception, Smith, and Low islands). During the area calculation processing, this split was necessary to stay within the cloud processing capacity-free quota designated for research. All the subsets are available at https://github.com/elianafonseca/antarctic_vegetation_map.

A unique NDVI maximum value composite image was generated using all the available images between January and April for the analyzed period (2016 – 2021). The austral summer months are related to the vegetation growing season in the Antarctic environment (Alberdi et al. 2002, Elster 2002, Lewis-Smith 2007, Selkirk & Skotnicki 2007). As we are using only images acquired during the summer months, the influence of different acquisition geometries due to the solar angle is minimized over the time series, which also reduces the effect of topographic shadows in vegetated pixels. To avoid the influence of cloud and snow pixels on NDVI values, a maximum value composite image was computed using all the available images collected over the area from January 1 to April 30 (1,861 over the northern part of the Antarctica Peninsula and 2,174 over the South Shetlands) in 2016–2021. This approach was necessary because we detected that Sentinel-2 cloud and ice-snow mask filters could not work correctly over this region, regardless of whether they are built using the QA60 band or QA10 and QA20 bands. When these masks were applied over a Sentinel-2 image collected over the Antarctic Peninsula and South Shetlands, it masked all image pixels, returning only empty pixels for all regions instead its TOA reflectance values.

The NDVI maximum value composite image had its values sliced into 21 bins; the first bin for the negative and positive values was sliced for each 0.05 until 1. The NDVI classes were labeled as mosses, lichens, or algae for generating the vegetation map based on the analysis made over Harmony Point. These reflectance patterns were used as criteria for separating mosses and lichens based on patterns described by Lovelock & Robinson (2002), Zhang et al. (2007), and Chi et al. (2021). The vegetation maps were validated by comparing results from Andrade et al. (2018) and Sun et al. (2021) over the Fildes Peninsula

and Ardley Island and with Shin et al. (2014) over the Barton Peninsula. For these analyses, a vegetation map for each analyzed year (2016–2021) was also computed, being the NDVI maximum value composite image from January 1 to April 30 for each year. A spectral profile for each vegetation class was constructed with the TOA reflectance average for each spectral band. The samples were collected over 20 points collected randomly in each vegetation class defined over the final vegetation map. These profiles allow us to identify better the “Top of Atmosphere Reflectance” patterns for mosses, lichens and algae in the Antarctic environment in the Sentinel-2 images.

Monthly meteorological data, such as total precipitation, mean air temperature, and total net shortwave radiation, were used to analyze the differences between mapped areas over different subsets (Tables I and II). These datasets were obtained using the GEE from the “ERA5_LAND/MONTHLY” collection, which provides aggregated values for each month from ECMWF/ERA5 climate reanalysis, using the same eleven subsets used to generate the vegetation maps.

Ocean/land mask generation

For automatic vegetation mapping, masking the ocean areas is required once the phytoplankton in the ocean also makes photosynthesis, and it can be mapped as vegetation, as observed by Fretwell et al. (2011). An alternative is to build a mask to process the satellite images acquired only over terrestrial areas, including the continent and the islands. The vector edges of the terrestrial areas from the Antarctic Digital Database - Quantarctica packaged (Matsuoka et al. 2021) were generated using a small cartographic scale, so the edges have low detail levels and cannot be used to mask land areas. An alternative is to have a mask using the satellite information. So, an ocean/

Table I. Mean air temperature, total precipitation, and total net shortwave radiation from January to April over North Antarctic Peninsula subsets for the study period (2016-2021).

Subset	South Peninsula			North Peninsula			North Islands			West Islands		
	AT (°C)	P (mm)	NR (MJ m ⁻²)	AT (°C)	P (mm)	NR (MJ m ⁻²)	AT (°C)	P (mm)	NR (MJ m ⁻²)	AT (°C)	P (mm)	NR (MJ m ⁻²)
2016	-7.0	830	8.1	-4.2	602	7.8	-3.0	438	8.7	-5.2	474	11.9
2017	-6.2	538	7.9	-3.7	434	7.3	-2.7	322	7.9	-4.7	349	11.2
2018	-5.7	1154	7.5	-3.0	870	7.2	-1.7	596	7.7	-4.4	593	10.1
2019	-7.0	779	8.1	-4.2	604	7.6	-2.9	413	8.0	-5.7	451	10.0
2020	-5.2	808	7.8	-2.8	595	7.4	-1.5	364	8.1	-3.7	307	11.3
2021	-5.5	1082	7.5	-2.8	732	7.3	-1.4	462	7.8	-3.9	405	10.5

* AT: mean air temperature, P: total precipitation, NR: total net shortwave radiation.

Table II. Mean air temperature, total precipitation, and total net shortwave radiation from January to April over South Shetlands islands subsets for the study period (2016-2021).

Subset	Elephant and Clarence			King George			Nelson			Robert			Livinstone			Deception		
	AT (°C)	P (mm)	NR (MJ m ⁻²)	AT (°C)	P (mm)	NR (MJ m ⁻²)	AT (°C)	P (mm)	NR (MJ m ⁻²)	AT (°C)	P (mm)	NR (MJ m ⁻²)	AT (°C)	P (mm)	NR (MJ m ⁻²)	AT (°C)	P (mm)	NR (MJ m ⁻²)
2016	-1.0	593	7.6	-1.3	694	8.6	-0.5	583	6.0	-0.5	588	5.6	-1.0	629	8.3	-0.3	596	5.5
2017	-0.4	483	9.0	-0.5	511	8.9	0.3	429	6.2	0.3	470	5.7	0.0	522	9.0	0.9	506	5.5
2018	0.4	598	9.8	0.0	787	8.6	0.7	686	5.8	0.7	723	5.4	0.1	778	8.7	0.9	785	5.5
2019	-0.7	600	10.5	-1.0	641	8.7	-0.2	540	6.3	-0.2	579	5.9	-0.6	640	8.5	0.2	641	5.7
2020	0.3	447	11.9	0.2	545	8.6	0.8	492	5.6	0.8	533	5.1	0.3	592	9.5	1.1	612	5.0
2021	0.4	652	10.3	0.1	783	7.9	0.8	656	5.4	0.7	685	5.0	0.2	793	9.5	0.9	774	5.0

* AT: mean air temperature, P: total precipitation, NR: total net shortwave radiation.

land mask was built over the area using the “water vapor band” (B9), centered at 945nm and 943.2nm for Sentinel 2A and 2B, with 60m spatial resolution. At these wavelengths, the liquid water reflectance is near zero, and the cloud and snow reflectance is around 0.7 (Jensen 2009). A minimum value composite image for B9 was computed for the entire area to generate the vegetation maps by selecting the minimum reflectance value registered for each pixel for the whole time series. With this approach, every water pixel acquired without ice or cloud cover, at least once during the time series, will be filled

with a TOA reflectance value near zero due to the water spectral reflectance pattern. The B9 minimum value composite image had its values remapped, building a binary image to identify the ocean and land areas.

RESULTS

Vegetation map

Over the Harmony point, the NDVI values associated with vegetated areas ranged from 0.15 to 0.8. Values lower than 0.15 were observed over the ice/snow areas and bare rocks. Table

I shows the surface reflectance values for the optical bands at the blue, green, red, and red edge, NIR, and SWIR wavelengths collected over each NDVI class.

Based on these analyses, the NDVI vegetation pixels were labeled algae when values were between 0.15 – 0.20, 0.20 – 0.50 for lichens, and 0.50 – 0.80 for mosses. The increase in reflectance values at the red edge and NIR wavelengths (Table III) was the criteria for separating mosses and lichens. The 17 sample points were overlapped on the NDVI sliced image to validate the NDVI labels. All four points collected during the fieldwork identified as algae vegetation samples presented lower NDVI values than other BSC (0.15 – 0.20). The six points which were collected over lichens areas were located over the mapped lichens classes (with NDVI values between 0.20 – 0.50), and the two points collected over mosses areas in the field were located over the mapped mosses classes (with NDVI values between 0.50 – 0.80). Five sample points were collected in areas with BSC mosaic cover, so they cannot be used to validate NDVI labels. On the other hand, considering that these points are over vegetation areas, all 17 points collected during the fieldwork were correctly mapped as vegetation using Sentinel-2 NDVI maximum value composite image, which validates our methodology for mapping vegetation with 100% accuracy.

The final vegetation map at its full spatial resolution (10 meters) can be accessed by running the provided link inside the GEE platform, where it is possible to observe the implementation code for the mask ocean/land pixels, the NDVI Maximum Value Composite calculation, its slicing and labeling (https://github.com/elianafonseca/antarctic_vegetation_map). Also, the vegetation map for the northern Antarctic Peninsula and South Shetlands at its full spatial resolution can be access using the

Earth Engine app interface, available at: <https://egee.scripts.users.earthengine.app/view/antarcticvegetationmap>.

The Figure 5 presents the TOA reflectance profiles for each vegetation class. The algae and lichens show the same patterns in the visible bands (B2, B3, B4 / 426-696nm) and we can be separated both due to their differences in the red edge (B5, B6, B7 / 688-800nm) and infrared (B8, B11, B12 / 727-2.371nm) bands. The mosses and lichens can easily separate based on the red edge bands (B5, B6, B7 / 688-800nm). Also, in this graph, we can observe the effects of the TOA reflectance, or reflectance without atmospheric correction, as a great reflectance in the blue wavelengths (B2 / 426-558nm), related to the blue scattering in the Troposphere.

The vegetation mapped areas are presented in Tables IV and V. Over the Antarctic Peninsula, 155.7 km² of vegetation area was mapped, and the algae are the most abundant vegetation type for all subsets (Table IV). Over South Shetlands, 60.4 km² of vegetation areas were mapped, and the lichens were the most abundant vegetation type among all subsets (Table V).

DISCUSSION

Despite the availability of a long-term Landsat image series collected over the Antarctic Region at official datasets repositories, those images still need geometric corrections. But in the Antarctic region, there are no features to identify in the satellite images to use as ground control points. The Sentinel-2 images are georeferenced using the Copernicus Precise Orbit Determination (POD) based on the satellite position at the acquired time. Thus, it solves the first fundamental problem of a satellite image time-series, the precise georeferencing for each image, which is essential for automatic data processing.

Table III. Mean surface reflectance values for each Sentinel-2 band collected over a Sentinel-2 image acquired on February 23, 2019, for each NDVI class at Harmony Point.

NDVI class interval	B2	B3	B4	B5	B6	B7	B8	B11	B12
0.15 - 0.20	0.12	0.14	0.14	0.16	0.18	0.18	0.20	0.21	0.16
0.20 - 0.25	0.08	0.10	0.11	0.13	0.15	0.16	0.18	0.25	0.17
0.25 - 0.30	0.07	0.09	0.10	0.13	0.15	0.17	0.19	0.27	0.18
0.30 - 0.35	0.07	0.09	0.10	0.13	0.16	0.18	0.20	0.27	0.18
0.35 - 0.40	0.07	0.09	0.10	0.13	0.17	0.19	0.21	0.29	0.19
0.40 - 0.45	0.06	0.09	0.10	0.13	0.17	0.20	0.22	0.29	0.19
0.45 - 0.50	0.06	0.08	0.09	0.13	0.18	0.21	0.24	0.31	0.20
0.50 - 0.55	0.05	0.08	0.09	0.13	0.19	0.22	0.25	0.31	0.20
0.55 - 0.60	0.05	0.08	0.08	0.13	0.20	0.24	0.28	0.32	0.20
0.60 - 0.65	0.04	0.07	0.07	0.13	0.22	0.25	0.30	0.33	0.20
0.65 - 0.70	0.04	0.07	0.07	0.14	0.25	0.30	0.36	0.33	0.20
0.70 - 0.75	0.03	0.07	0.06	0.14	0.27	0.32	0.38	0.32	0.19
0.75 - 0.80	0.03	0.06	0.06	0.13	0.26	0.32	0.37	0.29	0.17

* B2-Blue (426-558nm), B3-Green (523-595nm), B4-Red (634-696nm), B5-Red Edge (688-720nm), B6-Red Edge (724-754nm), B7-Red Edge (760-800nm), B8-NIR (727-939nm), B11-SWIR (1516-1705nm), B12-SWIR (2001-2371nm).

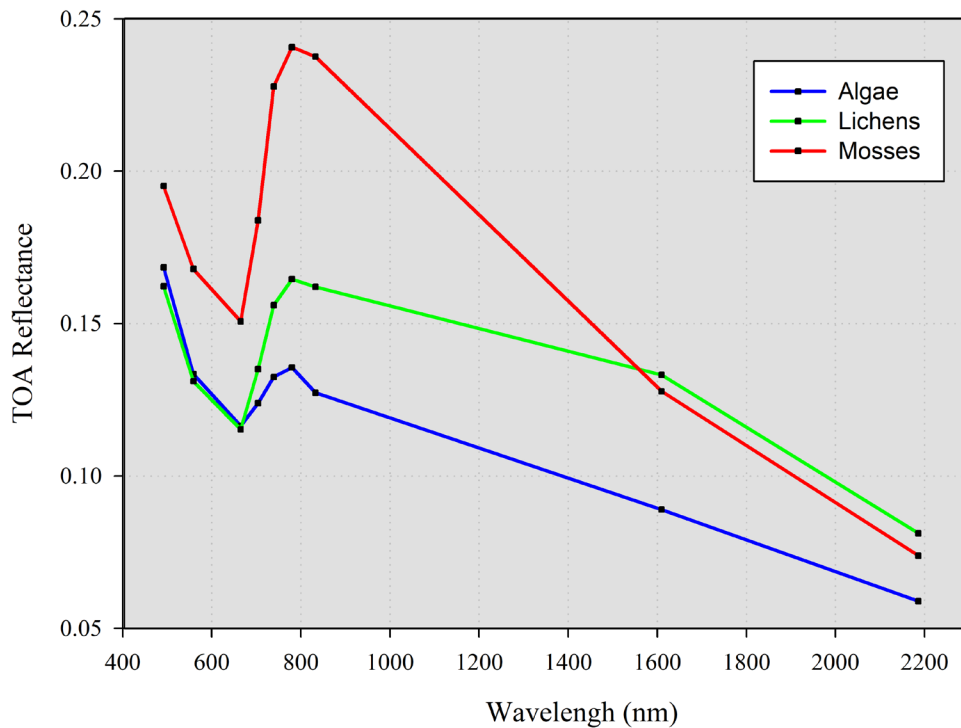


Figure 5. Sentinel-2 TOA reflectance profile patterns for algae, lichens and mosses in the Antarctic environment.

Table IV. Mapped vegetation areas (km²) for algae (AL), lichens (LI), and mosses (MO) over the Antarctic Peninsula subsets for the study period (2016-2021) and for the final vegetation map.

Subset ID*	NP_1			NP_2			NP_3			NP_4		
	AL	LI	MO	AL	LI	MO	AL	LI	MO	AL	LI	MO
2016	2.80	2.00	0.02	1.32	1.23	0.07	4.81	6.58	0.18	11.60	7.39	0.74
2017	0.57	0.24	0.00	0.85	0.44	0.00	3.11	4.29	0.02	3.06	0.97	0.00
2018	2.51	1.29	0.00	1.53	0.57	0.00	3.10	4.01	0.03	8.81	3.22	0.00
2019	1.48	2.17	0.01	1.24	0.86	0.00	4.47	4.85	0.16	8.23	4.82	0.07
2020	0.45	0.30	0.00	1.55	0.70	0.00	5.69	4.40	0.06	18.29	8.08	0.02
2021	2.96	1.72	0.01	3.81	2.14	0.01	9.44	5.80	0.01	30.99	18.52	0.08
Final map	9.26	6.21	0.04	8.37	4.51	0.08	16.15	12.54	0.40	64.81	32.43	0.88

* NP_1 south peninsula, NP_2 north peninsula, NP_3 north islands, NP_4 west islands.

Table V. Mapped vegetation areas (km²) for algae (AL), lichens (LI), and mosses (MO) over South Shetlands islands subsets for the study period (2016-2021) and for the final vegetation map.

Subset ID*	SS_1			SS_2			SS_3			SS_4			SS_5			SS_6			SS_7		
	AL	LI	MO																		
2016	0.25	0.11	0.00	1.94	3.45	0.06	0.67	1.60	0.02	1.33	2.74	0.05	1.56	1.69	0.01	0.62	0.51	0.00	0.99	0.92	0.00
2017	0.25	0.11	0.00	2.35	3.63	0.13	0.74	2.21	0.12	1.78	4.65	0.21	1.43	1.75	0.06	1.10	1.22	0.02	0.13	0.04	0.00
2018	1.24	1.64	0.02	2.18	4.89	0.28	0.71	2.27	0.15	1.19	3.55	0.26	0.28	0.21	0.00	0.08	0.09	0.00	0.54	0.64	0.00
2019	0.14	0.09	0.00	0.29	0.32	0.00	0.20	0.34	0.00	1.46	4.66	0.35	1.32	2.22	0.05	0.23	0.28	0.00	0.31	0.35	0.00
2020	1.24	0.93	0.01	2.49	5.67	0.29	0.85	2.23	0.14	1.63	4.91	0.34	2.28	3.73	0.06	0.31	0.40	0.00	0.70	0.92	0.01
2021	1.37	1.57	0.08	2.26	4.77	0.15	1.11	2.17	0.11	1.77	3.07	0.14	2.93	4.71	0.08	1.55	1.19	0.00	1.01	1.03	0.02
Final map	3.40	4.56	0.12	4.52	8.33	0.47	1.43	3.16	0.23	2.74	6.95	0.54	5.11	8.14	0.17	2.98	2.57	0.02	2.38	2.53	0.03

* SS_1: Elephant and Clarence, SS_2: King George, SS_3: Nelson, SS_4: Robert, SS_5: Livingston, SS_6: Deception, SS_7: Smith and Low.

Using the georeferenced Sentinel-2 time series with the NDVI maximum value composite approach in association with the ocean/land mask, we were able to eliminate the cloud and cloud-shadows pixels and exclude those pixels from phytoplankton over the ocean. These procedures allow the automatic process to generate the vegetation map.

The cloud computing process was essential to select, process, and analyze many images simultaneously. To generate the final vegetation map, 1,861 images acquired over the northern

part of the Antarctic Peninsula and 2,174 over the South Shetlands were used, automatically selected based on the date and region of interest over all images in the Sentinel-2 time series acquired worldwide. To generate the ocean/land mask all Sentinel-2 images available over Antarctica were used to compose the mask in a few seconds of processing. With these approaches, we were able to produce a regional vegetation map over the Antarctic continent and offshore islands. All the scientific workflow can be improved using more datasets,

like radar images, more knowledge to define the correct way to integrate different kinds of remotely sensed information, and also more computational time to process all the available data in order to generate a unique vegetation map over the entire Antarctic continent.

Vegetation map validation

The NDVI values associated with vegetated areas ranged from 0.15 to 0.8, agreeing with Fretwell et al. (2011) observations, who associated NDVI values higher than 0.20 with vegetation pixels in the Antarctic Peninsula using Landsat images. All four points collected during the fieldwork identified as algae vegetation samples presented lower NDVI values than other BSC (0.15 – 0.20), similar to the ones observed by Yun et al. (2017). Despite those agreements with other authors, the validation of our map was complex since there is no common Antarctic vegetation database or protocols for gathering information in this remote area. Also, the logistics for fieldwork are reduced (our team required 10-day fieldwork to collect 17 points dataset used to generate this vegetation map). So, the only way to validate the generated maps was by a qualitative comparison with other published maps.

Over the Barton Peninsula, Shin et al. (2014) mapped vegetation abundance using KOMPSAT-2 and QuickBird very-high-resolution images, reaching 0.72 for a global accuracy map. The spatial distribution of vegetation they found over this area had similar spatial distribution with the map generated in the present study. It indicates that our approach with Sentinel-2 images with 10m spatial resolution can map the vegetation over the Antarctic environment.

Over the Fildes Peninsula and Ardley Island, our vegetation map was compared with results from Sun et al. (2021), who estimated the areas dominated by mosses and lichens using field

measurements and spectral mixture analysis with a WorldView-2 image and with results from Andrade et al. (2018) who mapped the vegetation using a QuickBird image. Over Ardley Island, we estimate an area of 0.106 km² occupied by algae, 0.659 km² by lichens, and 0.212 km² by mosses. Sun et al. (2021) mapped lichens and mosses using visual image interpretation and estimated 0.3259 km² covered by mosses. Andrade et al. (2018) mapped two different classes, one for mosses (0.3165 km²) and the other for lichens and mosses association (0.3804 km²), using classification procedures with a global accuracy of 0.78. Some differences in mapped areas are expected due to the spatial resolution of the images, but, in many cases, the mosses distribution estimated with WorldView-2 (Sun et al. 2021) and QuickBird (Andrade et al. 2018) were mapped as algae when using Sentinel-2 images. Those authors did not identify this vegetation type, probably due to the low spectral resolution, characteristic of high spatial resolution images. Both mosses and algae occur in the same moist microenvironment (Becker 1982, Broady 1996, Lovelock & Robinson 2002), which can explain the difference observed in mapped areas. But, the spatial vegetation distribution determined over the Fildes Peninsula and Ardley Island by these authors was the same that we mapped, which indicates that our approach to mapping vegetation using Sentinel-2 images with 10m spatial resolution (B4 and B8) is valid with results similar to that obtained with very-high spatial resolution images.

The annual and spatial variations in mapped vegetation areas

The subsets used to calculate the vegetation areas have different dimensions; hence, a direct quantitative comparison among them is impossible. However, a high vegetation area mapped at the Antarctic Peninsula, subset NP_4

located over the west islands can be noticed (Table IV), similar to results from Fretwell et al. (2011) over the same region. Furthermore, it can be observed the greater total net shortwave radiation amount at this same subset (NP_4) than in other subsets (Table I), evidencing a microenvironment over this region that provided vegetation growth conditions. Zhou et al. (2021) also detected these microenvironment effects using remote sensing techniques to monitor environmental changes, such as dry-snow line variations. The microenvironment effects were pointed out as one of the driving forces to other environmental changes (*e.g.*, changes in phytoplankton communities; Ferreira et al. 2020) in the same region. Over the South Shetlands, no similar relationships between vegetation distribution and the weather variables or the geographic location were found in our results and the literature. These results show that the Sentinel-2 images can detect the spatial variations in the vegetation distribution over the Antarctic environment and generate valuable maps to use as input in environmental model simulations.

The annual variations in mapped vegetation areas observed among analyzed years (Tables IV and V) cannot be considered a land cover change in this region. As pointed out by Shin et al. (2014), some variations in vegetation abundance with the data acquisition month and interannual meteorological conditions are expected, but not for the vegetation distribution area since its expansion occur at a very slow rate in the Antarctic (Fritsen & Priscu 1998, Convey 2006). The differences in mapped vegetation areas for the Fildes Peninsula and Ardley Island over the years can be observed in Figure 6. Since no weather variations over the years were found over this area (Table II), these variations observed are, in fact, due to the cloud cover, which justifies the use of images acquired

in more than one year to build a valid vegetation map from Sentinel-2 images.

CONCLUSIONS

The Sentinel-2 images, with their 10m spatial resolution, allow the creation of valid vegetation maps for the Antarctica Peninsula and offshore islands, including the South Shetlands Islands. The availability of georeferenced satellite image datasets in cloud storage and ready to use in image processing was essential to process and analyze all the available data to generate a consistent and validated vegetation map over one of the most remote areas in the World. We can consider valid our methodology to map the vegetation cover over the Antarctic Peninsula and South Shetlands using a simple automatic process based on NDVI maximum value composite since the vegetation distribution mapped in this work was similar to literature maps in the same geographical areas. Also, the NDVI maximum value composite approach was necessary because the Sentinel-2 cloud and ice-snow mask filters could not work correctly over this region. The NDVI range between 0.15 – 0.80 is the ideal slice to identify the vegetation in the Antarctic environment using Sentinel-2 images. The NDVI values were associated with the occurrence of algae (0.15 – 0.20), lichens (0.20 – 0.50), and mosses (0.50 – 0.80). Due to the low frequency of cloud-free images over those regions, generating vegetation map distribution on an annual basis is challenging. The microenvironments which provide conditions for vegetation growth can be identified using the NDVI in association with the weather data in the Antarctic region. The ocean/land mask was essential to select only land pixels for this analysis, avoiding mapping the phytoplankton activity as vegetation photosynthesis, since the digital vector database was generated in a

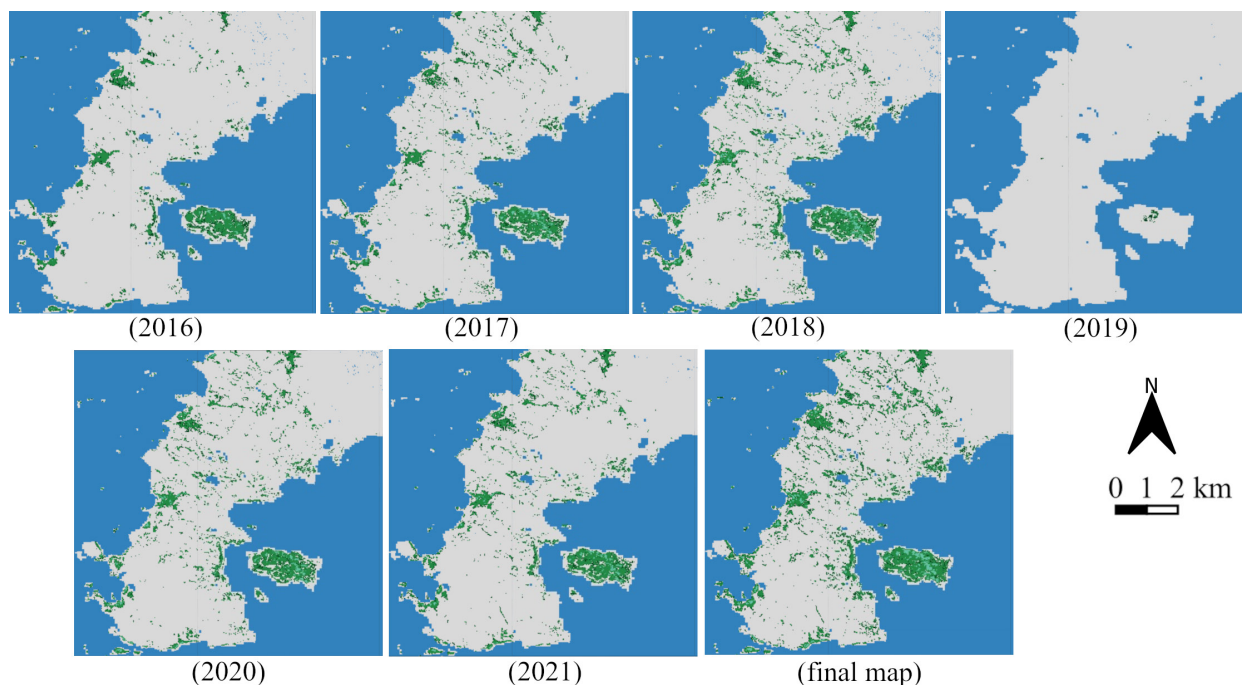


Figure 6. The annual vegetation distribution maps over Fildes Peninsula and Ardley Island for the study period (2016-2021) and for the final vegetation map.

coarse cartographic scale, which did not allow the identification of the correct shoreline border.

Acknowledgments

This work was supported financially by Conselho Nacional de Desenvolvimento Científico e Tecnológico (CNPq) - Process 465680/2014-3 and the Fundação de Amparo à pesquisa do Estado do Rio Grande do Sul (FAPERGS) - Process 17/25510000518-0 through the Brazilian National Institute for Cryospheric Sciences (INCT da Criosfera).

REFERENCES

ALBERDI M, BRAVO LA, GUTIÉRREZ A, GIDEKEL M & CORCUERA LJ. 2002. Ecophysiology of Antarctic vascular plants. *Physiol Plant* 115: 479-486.

ANDRADE AMD, MICHEL RFM, BREMER UF, SCHAEFER CEGR & SIMÕES JC. 2018. Relationship between solar radiation and surface distribution of vegetation in Fildes Peninsula and Ardley Island, Maritime Antarctica. *Int J Remote Sens* 39: 2238-2254.

BECKER EW. 1982. Physiological studies on Antarctic *Prasiola crispa* and *Nostoc commune* at low temperatures. *Polar Biol* 1: 99-104.

BÖLTER M, BEYER L & STONEHOUSE B. 2002. Antarctic coastal landscapes: characteristics, ecology and research. In: Beyer L & Bölter M (Eds), *Geocology of Antarctic ice-free coastal landscapes*, Berlin: Springer-Verlag, p. 5-15.

BROADY PA. 1996. Diversity, distribution and dispersal of Antarctic terrestrial algae. *Biodivers Conserv* 5: 1307-1335.

CALVIÑO-CANCELA M & MARTÍN-HERRERO J. 2016. Spectral Discrimination of Vegetation Classes in Ice-Free Areas of Antarctica. *Remote Sens* 8: 856.

CANNONE N, DALLE FRATTE M, CONVEY P, WORLAND MR & GUGLIELMIN M. 2017. Ecology of moss banks on Signy Island (maritime Antarctic). *Bot J Linn Soc* 184: 518-533.

CHI J, LEEH, HONG SG & KIM H-C. 2021. Spectral Characteristics of the Antarctic Vegetation: A Case Study of Barton Peninsula. *Remote Sens* 13: 2470.

CHOI SH, KIM SC, HONG SG & LEE KS. 2015. Influence of microenvironment on the spatial distribution of *Himantormia lugubris* (Parmeliaceae) in ASPA No. 171, maritime Antarctic. *J Ecol Environ* 38: 493-503.

- COLESIE C, WALSHAW CV, SANCHO LG, DAVEY MP & GRAY A. 2023. Antarctica's vegetation in a changing climate. *WIREs Climate Change* 14: e810.
- CONVEY P. 2006. Antarctic Terrestrial Ecosystems: Responses to Environmental Change. *Polarforschung* 75: 101-111.
- ELSTER J. 2002. Ecological classification of terrestrial algal communities in polar environments. In: Beyer L & Bölter M (Eds), *Geocology of Antarctic ice-free coastal landscapes*, Berlin: Springer-Verlag, p. 303-326.
- FERREIRA A, COSTA RR, DOTTO TS, KERR R, TAVANO VM, BRITO AC, BROTAS V, SECCHI ER & MENDES CRB. 2020. Changes in Phytoplankton Communities Along the Northern Antarctic Peninsula: Causes, Impacts and Research Priorities. *Front Mar Sci* 7: 576254.
- FRETWELL PT, CONVEY P, FLEMING AH, PEAT HJ & HUGHES KA. 2011. Detecting and mapping vegetation distribution on the Antarctic Peninsula from remote sensing data. *Polar Biol* 34: 273-281.
- FRIITSEN CH & PRISCU JC. 1998. Cyanobacterial assemblages in permanent ice covers on antarctic lakes: distribution, growth rate, and temperature response of photosynthesis. *J Phycol* 34: 587-597.
- GORELICK N, HANCHER M, DIXON M, ILYUSHCHENKO S, THAU D & MOORE R. 2017. Google Earth Engine: Planetary-scale geospatial analysis for everyone. *Remote Sens. Environ* 202: 18-27.
- JACOBA, KIRSTGO, WIENCKEC & LEHMANN H. 1991. Physiological responses of the Antarctic green alga *Prasiola crispa* ssp antarctica to salinity stress. *J Plant Physiol* 139: 57-62.
- JAWAK SD, LUIS AJ, FRETWELL PT, CONVEY P & DURAIRAJAN UA. 2019. Semiautomated Detection and Mapping of Vegetation Distribution in the Antarctic Environment Using Spatial-Spectral Characteristics of WorldView-2 Imagery. *Remote Sens* 11: 1909.
- JENSEN JR. 2009. *Remote sensing of the environment: An Earth resource perspective*. Upper Saddle River, NJ: Prentice Hall, 592 p.
- JUNG M ET AL. 2021. Areas of global importance for conserving terrestrial biodiversity, carbon and water. *Nat Ecol Evol* 5: 1499-1509.
- KAPPEN L. 2000. Some aspects of the great success of lichens in Antarctica. *Antarct Sci* 12: 314-324.
- KAPPEN L & SCHROETER B. 2002. Plants and Lichens in the Antarctic, Their Way of Life and Their Relevance to Soil Formation. In: Belnap J & Lange OL (Eds), *Biological soil crusts: structure, function, and management*. 150. Ecological Studies (Analysis and Synthesis). Berlin: Springer, p. 327-373.
- LEWIS-SMITH RI. 2007. Vegetation. In: Riffenburgh B (Ed), *Encyclopedia of the Antarctic*. New York: Taylor & Francis Group, p. 1033-1036.
- LOVELOCK CE & ROBINSON SA. 2002. Surface reflectance properties of Antarctic moss and their relationship to plant species, pigment composition and photosynthetic function: Surface reflectance of moss. *Plant Cell Environ* 25: 1239-1250.
- MATSUOKA K ET AL. 2021. Quantarctica, an integrated mapping environment for Antarctica, the Southern Ocean, and sub-Antarctic islands. *Environ Model Softw* 140: 105015.
- MIRANDA V, PINA P, HELENO S, VIEIRA G, MORA C & SCHAEFER CEGR. 2020. Monitoring recent changes of vegetation in Fildes Peninsula (King George Island, Antarctica) through satellite imagery guided by UAV surveys. *Sci Total Environ* 704: 135295.
- MONIZ MJB, RINDI F, NOVIS PM, BROADY PA & GUIRY MD. 2012. Molecular phylogeny of antarctic prasiola (prasiolales, trebouxioophyceae) reveals extensive cryptic diversity: cryptic diversity of antarctic prasiola. *J Psychol* 48: 940-955.
- PEAT HJ, CLARKE A & CONVEY P. 2007. Diversity and biogeography of the Antarctic flora. *J Biogeogr* 34: 132-146.
- SANCHO LG & PINTADO A. 2004. Evidence of high annual growth rate for lichens in the maritime Antarctic. *Polar Biol* 27: 312-319.
- SELKIRK PM & SKOTNICKI ML. 2007. Measurement of moss growth in continental Antarctica. *Polar Biol* 30: 407-413.
- SHIN J-I, KIM H-C, KIM S-I & HONG SG. 2014. Vegetation abundance on the Barton Peninsula, Antarctica: estimation from high-resolution satellite images. *Polar Biol* 37: 1579-1588.
- SOTILLE ME, BREMER UF, VIEIRA G, VELHO LF, PETSCH C & SIMÕES JC. 2020. Evaluation of UAV and satellite-derived NDVI to map maritime Antarctic vegetation. *Appl Geogr* 125: 102322.
- SUN X, WU W, LI X, XU X & LI J. 2021. Vegetation Abundance and Health Mapping Over Southwestern Antarctica Based on WorldView-2 Data and a Modified Spectral Mixture Analysis. *Remote Sens* 13: 166.
- WARREN MA, SIMIS SGH, MARTINEZ-VICENTE V, POSER K, BRESCIANI M, ALIKAS K, SPYRAKOS E, GIARDINO C & ANSPER A. 2019. Assessment of atmospheric correction algorithms

for the Sentinel-2A MultiSpectral Imager over coastal and inland waters. *Remote Sens. Environ* 225: 267-289.

YUN Z, RONG-LIANG J, YAN-HONG G, YUAN-YUAN Z & JIA-LING T. 2017. Characteristics of normalized difference vegetation index of biological soil crust during the succession process of artificial sand-fixing vegetation in the Tengger Desert, Northern China. *Chin J Plant Ecol* 41: 972-984.

ZHANG YM, CHEN J, WANG L, WANG XQ & GU ZH. 2007. The spatial distribution patterns of biological soil crusts in the Gurbantunggut Desert, Northern Xinjiang, China. *J Arid Environ* 68: 599-610.

ZHOU C, LIU Y & ZHENG L. 2021. Satellite-derived dry-snow line as an indicator of the local climate on the Antarctic Peninsula. *J Glaciol*: 1-11.

How to cite

FONSECA EL, SANTOS EC, FIGUEIREDO AR & SIMÕES JC. 2023. The use of sentinel-2 imagery to generate vegetations maps for the Northern Antarctic peninsula and offshore islands. *An Acad Bras Cienc* 95: e20230710. DOI 10.1590/0001-3765202320230710.

Manuscript received on June 25, 2023;
accepted for publication on November 16, 2023

ELIANA L. DA FONSECA¹

<https://orcid.org/0000-0002-9129-2939>

EDVAN C. DOS SANTOS²

<https://orcid.org/0000-0001-8008-2509>

ANDERSON R. DE FIGUEIREDO²

<https://orcid.org/0000-0002-0228-249X>

JEFFERSON C. SIMÕES^{1,3}

<https://orcid.org/0000-0001-5555-3401>

¹Universidade Federal do Rio Grande do Sul, Centro Polar e Climático, Departament of Geography, Av. Bento Gonçalves, 9500, Bairro Agronomia, 91501-970 Porto Alegre, RS, Brazil

²Universidade Federal do Rio Grande do Sul, Centro Polar e Climático, Av. Bento Gonçalves, 9500, Bairro Agronomia, 91501-970 Porto Alegre, RS, Brazil

³University of Maine, Climate Change Institute, 04469-5790, Orono, ME, USA

Correspondence to: **Eliana Lima da Fonseca**

E-mail: eliana.fonseca@ufrgs.br

Author contributions

ELF performed the fieldwork, analyzed the data, wrote, reviewed, and edited the manuscript; ECS performed the literature review, analyzed the data, and wrote the manuscript; ARF performed the fieldwork; JCS reviewed the manuscript and acquired the financial resources for this investigation. All authors discussed the results and approved the final version of the manuscript.

